ISSN 0915-633X

NATIONAL INSTITUTE FOR FUSION SCIENCE

Shift-and-Inverse Lanczos Algorithm for Ideal MHD Stability Analysis

J. Chen, N. Nakajima, M. Okamoto

(Received - Oct. 21, 1997)

NIFS-518 Nov. 1997

RESEARCH REPORT
NIFS Series

NAGOYA, JAPAN

Shift-and-Inverse Lanczos Algorithm for Ideal MHD Stability Analysis

J.Chen[a,1], N.Nakajima[b], M.Okamoto[b]
[a]Graduate University for Advanced Studies
[b]National Institute for Fusion Science, 322-6, Oroshi-cho, Toki, Gifu 509-52, Japan

Abstract

CAS3D and TERPSICHORE have been designed to analyze the global ideal MHD stability of three dimensional equilibria. Their critical part is to obtain the smallest eigenvalue and its corresponding eigenvector of a large but sparse real symmetric band matrix. In CAS3D the inverse iteration have been applied to do this and the spectral shift is computed by EISPACK eigensolver. It has been shown that application of such kind of software becomes very expensive in the sense of computational time and storage when matrix order and bandwidth become very large. Here this problem is resolved by using the Lanczos algorithm which is economical in CPU time and storage and particularly suitable for very large scale problems. The version of CAS3D2MN with shift-and-inverse Lanczos algorithm is called CAS3D2MNv1. Practical calculations in CAS3D2MNv1 indicate that the shift-and-inverse Lanczos recursion needs only $15 \sim 20$ steps to calculate the smallest eigenvalue. The computation is reliable and efficient. The storage is much smaller and CPU time is saved significantly by $50 \sim 100$ times compared with EISPACK subroutine. Finally the ballooning mode in three dimensional MHD equilibria has been mentioned briefly.

Keywords: Lanczos recursion with no re-orthogonalization, shift-and-inverse Lanczos recursion, Lanczos Phenomenon, gap stiffness, CAS3D2MN, CAS3D2MNv1.

[1]e-mail: jchen@tadws06.nifs.ac.jp fax: (81) 0572-58-2630

1 Introduction

One of the important part in ideal MHD stability analysis is to solve the eigenproblem (e.g. CAS3D [1] and TERPSICHORE [2])

$$\boldsymbol{P}\boldsymbol{x} = \bar{\lambda}\boldsymbol{K}\boldsymbol{x} \tag{1.1}$$

where $\boldsymbol{P}$ and $\boldsymbol{K}$, arising from finite element approximation and Fourier decomposition, are potential and kinetic energy, respectively. Both are symmetric matrices. Furthermore, $\boldsymbol{K}$ is positive definite. By non-physical normalization Eq.(1.1) can be converted into

$$\boldsymbol{A}\boldsymbol{x} = \lambda\boldsymbol{x} \tag{1.2}$$

as is done in CAS3D [1]. $\boldsymbol{A}$ is a large but sparse real symmetric matrix with order n and upper half bandwidth b, $b \ll n$. In our applications, n is from 8435 to 120081 and b from 104 to 602. The set $(\lambda, \boldsymbol{x})$ is called the eigenelement of $\boldsymbol{A}$.

In CAS3D and TERPSICHORE, the following inverse iteration (see e.g. [3])

$$\begin{array}{ll} \text{for} & k = 1.2, \ldots \\ & \text{Solve } (\boldsymbol{A} - ewshift\ \boldsymbol{I})\boldsymbol{z}^k = \boldsymbol{x}^{k-1} \\ & \boldsymbol{x}^k = \boldsymbol{z}^k / \|\boldsymbol{z}^k\|_2 \\ & \lambda^k = \boldsymbol{x}^{kT}\boldsymbol{A}\boldsymbol{x}^k \\ \text{end} & \end{array} \tag{1.3}$$

has been applied to calculate the smallest eigenvalue and its corresponding eigenvector, in which the spectral shift $ewshift$ in Eq.(1.3) is given by EISPACK [4] subroutine (for CAS3D):

$$ewshift = \lambda_{min} \text{ (by EISPACK subroutine)} \tag{1.4}$$

But EISPACK eigensolver is not suitable for eigenproblems of very large but sparse matrices such as in CAS3D2MN in the following three aspects:

- the given matrix will be modified during the computation and fill-ins are inevitably brought in. So its sparsity will be destroyed.
- $O(n^3)$ operations are needed to run because of application of the orthogonal similarity transformation.
- $O(n^2)$ words must be specified for storage.

which greatly limit the size of problems we can handle.

In our calculations, when the radial grid points increase from 120 to 300 and Fourier harmonic number from 35 to 201, respectively, the EISPACK and LAPACK [5] routines have failed to calculate $ewshift$ in 10 hours on SX system at NIFS. So it is natural for us to consider Lanczos recursion without re-orthogonalization which supersedes the above softwares:

- The given matrix $\boldsymbol{A}$ enters the recursion only through the matrix-vector multiplies $\boldsymbol{Ax}$ and its sparsity will not be modified during the calculation.
- For a sparse matrix, operations required to generate the Lanczos matrices using the recursion without re-orthogonalization is $O(n^2)$. and storage requirements is just $O(n)$.

It is just the above advantage that makes the Lanczos algorithm without re-orthogonalization be particularly suitable for and extensively applied to very large and sparse matrix problems [6-13].

In fact in our experiences. the smallest eigenvalue computed by Lanczos recursion without re-orthogonalization is as accurate as the value after inverse

iteration and we can replace the inverse iteration in original code CAS3D2MN by directly calculating its corresponding eigenvector of Lanczos matrix $\boldsymbol{T}_m$ and then calculating the Ritz vector of original matrix $\boldsymbol{A}$. But here we don't want to do so, since the required CPU time in inverse iteration is much smaller than that in $ewshift$ estimation when $ewshift$ provides a good approximation to the smallest eigenvalue.

We use the standard notation to distinguish scalars (lower-case italic letters), vectors (lower-case bold letters) and matrices (upper-case bold letters). All quantities are real and the only norm we use is the Euclidean norm

$$\|\boldsymbol{q}\| = \sqrt{\boldsymbol{q}^T\boldsymbol{q}}, \quad \|\boldsymbol{A}\| = \sup_{\|\boldsymbol{q}\|=1} \|\boldsymbol{A}\boldsymbol{q}\| \tag{1.5}$$

2 Lanczos Algorithm without Re-orthogonalization

The Lanczos recursion is a method for replacing the eigenproblem of a given symmetric matrix $\boldsymbol{A}$ by eigenproblems on a series of simpler Lanczos tridiagonal matrices, given as $\boldsymbol{T}_m$. Subsets of eigenvalues of these tridiagonal matrices are selected as approximate eigenvalues of the given matrix $\boldsymbol{A}$. Their approximation accuracy depends on the magnitude of the last component of the corresponding eigenvectors of $\boldsymbol{T}_m$ as long as the eigenvalues being considered are isolated eigenvalues of the associated Lanczos matrix.

Let $\boldsymbol{A}$ be a real, symmetric matrix of order n. Its corresponding Lanczos matrices can be given by the following recursion, which is highly recommended by Paige [6] and widely used [7-13] due to finite computer precision. Define $\beta_1 \equiv 0$ and $\boldsymbol{q}_0 \equiv 0$, and choose $\boldsymbol{q}_1$ as a random vector with $\|\boldsymbol{q}_1\| = 1$. Then for $i = 1, 2, \ldots, m$ define Lanczos vectors $\boldsymbol{q}_i$ and scalars α_i and β_{i+1} by

$$\begin{aligned} \beta_{i+1}\boldsymbol{q}_{i+1} &= \boldsymbol{A}\boldsymbol{q}_i - \beta_i\boldsymbol{q}_{i-1} - \alpha_i\boldsymbol{q}_i \\ \alpha_i &= \boldsymbol{q}_i^T(\boldsymbol{A}\boldsymbol{q}_i - \beta_i\boldsymbol{q}_{i-1}) \\ |\beta_{i+1}| &= \|\boldsymbol{A}\boldsymbol{q}_i - \beta_i\boldsymbol{q}_{i-1} - \alpha_i\boldsymbol{q}_i\| \\ \|\boldsymbol{q}_{i+1}\| &= 1 \end{aligned} \tag{2.1}$$

The $\alpha_i\boldsymbol{q}_i$ and the $\beta_i\boldsymbol{q}_{i-1}$ are, respectively, projection of $\boldsymbol{A}\boldsymbol{q}_i$ onto $\boldsymbol{q}_i$ and $\boldsymbol{q}_{i-1}$.

For each m, the corresponding Lanczos matrix $\boldsymbol{T}_m$ is defined as the real symmetric and tridiagonal matrix

$$\boldsymbol{T}_m = \begin{bmatrix} \alpha_1 & \beta_2 & & & & \\ \beta_2 & \alpha_2 & \cdot & & & \\ & \cdot & \cdot & \cdot & & \\ & & \cdot & \cdot & \cdot & \\ & & & \cdot & \alpha_{m-1} & \beta_m \\ & & & & \beta_m & \alpha_m \end{bmatrix} \tag{2.2}$$

in compact form

$$\boldsymbol{A}\boldsymbol{Q}_m = \boldsymbol{Q}_m\boldsymbol{T}_m + \beta_{m+1}\boldsymbol{q}_{m+1}\boldsymbol{e}_m^T \tag{2.3}$$

where $\boldsymbol{Q}_m = [\boldsymbol{q}_1, \boldsymbol{q}_2, \ldots \boldsymbol{q}_m]$ and $\boldsymbol{e}_m^T = (0, \ldots, 0, 1)$. Thus, given a real symmetric matrix $\boldsymbol{A}$ and a starting vector $\boldsymbol{q}_1$, the Lanczos recursion generates a family of real symmetric tridiagonal matrices related to $\boldsymbol{A}$ and to $\boldsymbol{q}_1$ through (2.3). So problem (1.2) is equivalent to solve

$$\boldsymbol{T}_m\boldsymbol{y} = \mu\boldsymbol{y} \tag{2.4}$$

where the set $(\mu, \boldsymbol{y})$ corresponds to the eigenpair of the Lanczos matrix $\boldsymbol{T}_m$. Clearly only

- storage for generating the matrix-vector multiplies $\boldsymbol{A}\boldsymbol{q}_i$,
- storage for only two Lanczos vectors $\boldsymbol{q}_i$ and $\boldsymbol{q}_{i-1}$ of length n,
- space for the tridiagonal Lanczos matrix $\boldsymbol{T}_m$ itself.

should be specified, and arithmetic operations mainly come from calculating $\boldsymbol{A}\boldsymbol{q}_i$. So the operation counts just grow as the square of n and the storage requirements are just a linear function of n when matrix is very sparse. In CAS3D2MN the ratio of zero entries to non-zero entries is about $n/2b$ (usually 100) and the matrix is very sparse. Thus the square dependence of arithmetic operations and linear dependence of storage requirements allow us to work with sufficient large problems needed by MHD stability analysis.

Our implementation of the above recursion is based upon the following fact called Lanczos Phenomenon:

Given any real symmetric matrix $\boldsymbol{A}$, then for large enough m,
every distinct eigenvalue of $\boldsymbol{A}$ will be an eigenvalue of $\boldsymbol{T}_m$.

and the identification test:

the convergence of the eigenvalues of the
Lanczos matrices as the size m is increased.

We choose the necessary number of Lanczos steps m automatically. Suppose μ' and μ'' are the smallest eigenvalues of successive Lanczos matrices $\boldsymbol{T}_{m'}$ and $\boldsymbol{T}_{m''}$ ($m' \neq m''$). If the difference $|\mu' - \mu''|$ between μ' and μ'' is smaller than the given convergence tolerance, we then set $\mu = \mu' = \mu'', m = m''$ and compute the magnitude of mth component $\boldsymbol{y}(m)$ of μ's eigenvector $\boldsymbol{y}$ (of $\boldsymbol{T}_m$). This is according to Paige [1980] (see e.g. [7]):

For a given m and for any isolated eigenvalue μ of the Lanczos

matrix $\boldsymbol{T}_m$, there exists an eigenvalue λ of $\boldsymbol{A}$ such that

$$|\lambda - \mu| \leq 2.5[|\beta_{m+1}\boldsymbol{y}(m)|(1+2\epsilon_0) + 2\epsilon_1\|\boldsymbol{A}\|m^{1/2}] \tag{2.5}$$

where ϵ_0 and ϵ_1 are related to machine precision ϵ. and satisfy $4m(3\epsilon_0+\epsilon_1) \ll 1$. The term $\epsilon_\mu \equiv |\beta_{m+1}\boldsymbol{y}(m)|$ plays the key role in estimating the convergence of computed eigenvalue μ. That is, if the last component $\boldsymbol{y}(m)$ is very small, eigenvalue μ will be a good approximation of eigenvalue λ of $\boldsymbol{A}$.

We use inverse iteration (1.3) to compute $\boldsymbol{y}(m)$ of the corresponding Lanczos matrix $\boldsymbol{T}_m$. In our experiences, the above μ will be as accurate as what have been computed by EISPACK or LAPACK subroutine. At each iteration only the incremental scalars α_i, β_{i+1} have to be generated. The Lanczos recursion with no re-orthogonalization can be given as:

- step 1. Specify an initial Lanczos step $m \ll n$, increase step $k > 0$, and convergence tolerances $CONTOL1$ and $CONTOL2$.
- step 2. Putting $m = m + k$, generate the real symmetric tridiagonal matrix $\boldsymbol{T}_m$ by recursion (2.1) and keep $\boldsymbol{q}_m$ and $\boldsymbol{q}_{m+1}$ for next iteration.
- step 3. Compute the smallest eigenvalue μ of the Lanczos matrix $\boldsymbol{T}_m$.
- step 4. Select μ which appeares in successive $\boldsymbol{T}_m$ by $CONTOL1$ and compute its convergence by inverse iteration method (1.3).
- step 5. If convergence is observed by $CONTOL2$, accept μ as the approximation of λ_{min} of the given matrix $\boldsymbol{A}$ and terminate. Otherwise, go to step 2 to enlarge $\boldsymbol{T}_m$.

In CAS3D2MN, the matrix $\boldsymbol{A}$ is indefinite. Its negative eigenvalues indicate MHD instability. However. $\boldsymbol{A}$ is rich in positive eigenvalues with magnitude as large as $\sim 10^6$. The number of negative eigenvalues is few and their magnitudes are as small as $\sim 10^{-3}$. Particularly, these matrices have gap stiffness behaving like what Cullum and Willoughby called the worst case [8]. Here the large positive eigenvalues rather than the negative eigenvalues are dominant. Recursion (2.1) converges very slowly by direct application to $\boldsymbol{A}$. But this recursion is accelerated significantly by shift-and-inverse recursion which is the topic of the next section.

3 shift-and-inverse Lanczos Algorithm

In CAS3D2MN, the bad gap stiffness slows down the convergence of desired eigenvalues when the Lanczos recursion (2.1) is applied directly on $\boldsymbol{A}$. This leads us to apply the Lanczos recursion (2.1) to $\boldsymbol{A}^{-1}$. With this transformation, the desired part of spectrum becomes dominant. The Lanczos recursion is accelerated in the sense that the size of the Lanczos matrix required to obtain the desired eigenvalues is much smaller.

Since it is not wise to work directly with such a poorly-conditioned matrix, we used the better-conditioned, positive definite, scaled and shifted matrix:

$$\boldsymbol{C} = (\boldsymbol{A} + SHIFT\ \boldsymbol{I})/S0 \tag{3.1}$$

$SHIFT$ is carefully chosen to shift $\boldsymbol{A}$ to be a positive definite matrix and $S0$ is used to scale the given matrix $\boldsymbol{A}$. The sparsity of $\boldsymbol{C}$ is the same as that of $\boldsymbol{A}$ and the eigenvalues of $\boldsymbol{A}$ can be easily obtained from those of $\boldsymbol{C}$ by performing sparse Cholesky factorization

$$\boldsymbol{C} = \boldsymbol{U}^T\boldsymbol{U} \tag{3.2}$$

Here $\boldsymbol{C}$ is overwritten with upper triangular matrix $\boldsymbol{U}$ which has the same upper bandwidth as $\boldsymbol{C}$. Then for any given vector $\boldsymbol{q}$, the vector $\boldsymbol{p} = \boldsymbol{C}^{-1}\boldsymbol{q}$ can be evaluated efficiently by solving sequentially two triangular systems of equations

$$\boldsymbol{U}^T\boldsymbol{U}\boldsymbol{p} = \boldsymbol{q}: \qquad \boldsymbol{U}^T\bar{\boldsymbol{p}} = \boldsymbol{q}. \qquad \boldsymbol{U}\boldsymbol{p} = \bar{\boldsymbol{p}} \tag{3.3}$$

The shift-and-inverse Lanczos algorithm can be formed as follows:

$\boldsymbol{C} = \boldsymbol{U}^T\boldsymbol{U}$(Cholesky factorization of $\boldsymbol{C}$)
Put $\boldsymbol{q}_0 = 0, \beta_0 = 0.$ and choose $\boldsymbol{q}_1$ as a random vector with $\|\boldsymbol{q}_1\| = 1$
For $i = 1$ to m do
$\boldsymbol{q} = \boldsymbol{q}_i$
$\boldsymbol{U}^T\boldsymbol{p} = \boldsymbol{q}$
$\boldsymbol{U}\boldsymbol{q} = \boldsymbol{p}$
$\boldsymbol{q} = \boldsymbol{q} - \beta_{i-1}\boldsymbol{q}_{i-1}$
$\alpha_i = \boldsymbol{q}_i^T\boldsymbol{q}$
$\boldsymbol{q} = \boldsymbol{q} - \alpha_i\boldsymbol{q}_i$
$\beta_i = \|\boldsymbol{q}\|$
if $(\beta_i = 0)$ then
    $\boldsymbol{q}_{i+1} = 0$
    stop
else
    $\boldsymbol{q}_{i+1} = \boldsymbol{q}/\beta_i$
endif

(3.4)

Although each step using $\boldsymbol{C}^{-1}$ is more expensive than a corresponding step using $\boldsymbol{A}$, the large decrease in the number of Lanczos steps required and the fact that the factors are also sparse, yield overall large gains in storage and time. The convergence is sped up remarkably by working with $\boldsymbol{C}^{-1}$ rather than directly with $\boldsymbol{A}$. The smallest eigenvalue has been computed in only $15 \sim 20$ Lanczos steps.

Suppose $(\mu, \boldsymbol{y})$ is an eigenpair of $\boldsymbol{T}_m$. i.e. $\boldsymbol{T}_m \boldsymbol{y} = \mu \boldsymbol{y}$, then

$$\|[(\boldsymbol{A} - SHIFT\ \boldsymbol{I})/S0]^{-1}\boldsymbol{Q}_m\boldsymbol{y} - \mu\boldsymbol{Q}_m\boldsymbol{y}\| = |\beta_{m+1}\boldsymbol{y}(m)| \tag{3.5}$$

and the eigenvalue λ of $\boldsymbol{A}$ can be evaluated as

$$\boldsymbol{A}\boldsymbol{x} = \lambda\boldsymbol{x} \Longleftrightarrow [(\boldsymbol{A} - SHIFT\ \boldsymbol{I})/S0]^{-1}\boldsymbol{x} = [(\lambda - SHIFT)/S0]^{-1}\boldsymbol{x} \tag{3.6}$$

so

$$(\lambda - SHIFT)/S0 = \mu^{-1} \tag{3.7}$$

that is

$$\lambda = S0/\mu + SHIFT \tag{3.8}$$

4 Application

The original Lanczos recursion given by (2.1) and the shift-and-inverse Lanczos recursion given by (3.4) both have been applied to solve the eigenvalue problem resulting from the ideal MHD stability analysis in a three dimensional MHD equilibrium. As an equilibrium, $L/N_T = 2/10$ planar axis equilibrium like one in the Large Helical Device (LHD)[14] is used where L and N_T are the polarity and the toroidal field period of the helical coils. respectively.

As is mentioned in Refs.[15] and [16] by using high-mode-number analysis of the ballooning modes, there are two types of ballooning modes in such three dimensional equilibria. One is tokamak-like ballooning mode with a weak three dimensional effect (a weak toroidal coupling), and the other is inherent to the three dimensional equilibria, and has not only strong poloidal

couplings but also strong toroidal couplings. The former's level surfaces of the unstable eigenvalues λ are topologically cylindrical in (ψ, θ_k, α) space, and the latter's level surfaces are topologically spheroidal in (ψ, θ_k, α), where ψ and α are labels of the flux surfaces and magnetic field lines, respectively, and θ_k is the radial wave number coming from the eikonal approximation. As is well known, there is no α-dependence of λ in axisymmetric tokamaks. In the strongly Mercier unstable three dimensional equilibria, high-mode-number ballooning modes with cylindrical level surfaces of λ and modes with spheroidal level surfaces of λ coexist. In contrast with it, in the slightly Mercier unstable or completely Mercier stable equilibria, only high-mode-number ballooning modes with spheroidal level surfaces of λ exist.

To check the performance of the Lanczos recursion methods given by Eqs.(2.1) and (3.4), a strongly Mercier unstable equilibrium is used. Since the used three dimensional equilibrium has $N_T = 10$ field period in the toroidal direction, there are six mode families, i.e., $N_f = 0, 1, \ldots, 5$[1]. In our calculations, the perturbation is taken to belong to $N_f = 5$ mode family and the phase factor, which is used in order to select the Fourier modes of the perturbation in the desired Fourier space[1], is chosen to be $(M, N) = (8, -5)$.

At first, in order to clarify the properties of the matrix in Eq.(1.2), we state the definition of gap stiffness and matrix stiffness [7] which greatly affects the convergence of Lanczos recursion.

Definition. For a real symmetric matrix $\boldsymbol{A}$ with distinct eigenvalues $\lambda_{k_1} > \lambda_{k_2} > \cdots > \lambda_{k_s}$, define the minimal gap g_j for each eigenvalue $\lambda_{k_j}, 1 \leq j \leq s$ as follows:

$$
\begin{aligned}
g_1 &\equiv (\lambda_{k_1} - \lambda_{k_2}) \\
g_s &\equiv (\lambda_{k_s} - \lambda_{k_{s-1}}) \\
g_j &\equiv min[\lambda_{k_j} - \lambda_{k_{j+1}}, \lambda_{k_{j-1}} - \lambda_{k_j}], \text{ for } j = 2, \ldots s-1
\end{aligned} \tag{4.1}
$$

The overall gap stiffness is defined by

$$
S_g(\boldsymbol{A}) \equiv \max_j g_j / \min_j g_j \tag{4.2}
$$

and the matrix stiffness by

$$
S(\boldsymbol{A}) \equiv \max_j |\lambda_j| / \min_j |\lambda_j| \tag{4.3}
$$

As the gap stiffness increases, the degree of difficulty in computing the desired part of spectrum with small gaps increases.

The overall MHD spectrum is given in Fig.1, where the number of the Fourier modes of the perturbation L and the number of the radial meshes NS are 35 and 120, respectively. The positive eigenvalues are clearly dominant and the left half of them are much more larger in amplitude compared with the right half part. From left to right, eigenvalues decrease monotonically. The most right end is magnified and we can see only a few negative eigenvalues.

The eigenvalues have been scaled by the function $\sinh^{-1}(\alpha x)$ with $\alpha = 10^5$ in Fig.2. The gap stiffness corresponding to Figs.1 and 2 is shown in Fig.3. The stiffness is so locally distributed at the left half part that it is difficult to distingush the stiffness of each eigenvalue. The right end stiffness, which is also magnified, is very small. This is the reason why the original Lanczos recursion given by Eq.(2.1) does not work well. In the parameters used in Figs.1-3, it has taken us as much as $2n$ steps to obtain the negative eigenvalues and $11n$ steps to obtain the smallest eigenvalue, where n is the matrix order. Obviously, it is the location of desired eigenvalues in the spectrum, the local separation of eigenvalues, and primally the overall gap stiffness of matrix $\boldsymbol{A}$ which determine the convergence of the desired eigenvalues as the size m of $\boldsymbol{T}_m$ is increased.

This original Lanczos recursion is sped up significantly by introducing a shift and using the inverse of the shifted matrix in the recursion, namely, by the shift-and-inverse Lanczos recursion given by Eq.(3.4). The storage is same but CPU time has been decreased considerably. The comparison of the shift-and-inverse Lanczos recursion with EISPACK and LAPACK routines is given in Table 1 for calculating the smallest eigenvalues. Only the number of Fourier modes L and the number of the radial meshes NS are changed as shown in the first column in Table 1, which leads to the variation of the matrix order n and upper half bandwidth b. The $SHIFT$ in Eq.(3.1) is chosen to be 0.01. From the second column to the sixth column, the smallest eigenvalue, the matrix order, the storage[2], the CPU time, and the speedup rate of the recursion (3.4) compared to EISPACK are shown. The name of algorithm is marked at the right end of the Table, for which the data in the same row have been used. From the table we can see that LAPACK subroutine has relatively smaller storage requirement but more CPU time compared with EISPACK. For shift-and-inverse Lanczos recursion (3.4), usually $15 \sim 20$ Lanczos steps are enough. That is, the smallest eigenvalue of Lanczos tridiagonal matrix $\boldsymbol{T}_m$ with order $15 \sim 20$ is a good approximation of $\boldsymbol{A}$'s smallest eigenvalue. Its storage requirement is much smaller compared with EISPACK and LAPACK, and $50 \sim 100$ times of speedup are achieved easily. In the final part of the table where NS is increased upto 300 and L upto 201, EISPACK and LAPACK have failed to calculate λ_{min} in 10 hours, but for recursion (3.4) only 903sec are sufficient. From this point, the shift-and-inverse Lanczos recursion (3.4) is a quite efficient tool in MHD stability analysis where EISPACK or LAPACK software may fail.

[2]The storage requirement is mainly determined by matrix order and bandwidth. Storage size for EISPACK is an approximate value but there is only a little difference.

Figure 4 is the radial structure of the ballooning mode in the strongly Mercier unstable three dimensional equilibria, where $N_f = 1$ mode family is used with the phase factor $(M, N) = (133, -77)$ [1]. radial mesh $NS = 600$, Fourier harmonics $L = 273$, and $\lambda_{min} = -1.0991 \times 10^{-2}$. Storage requirement by CAS3D2MNv1 is 1.178GB and CPU time for λ_{min} is about 721sec while EISPACK or LAPACK can not perform. In Figure 4. we can see different toroidal mode number coupling to creat ballooning mode in the three dimensional MHD equilibria.

5 Conclusion

The Lanczos algorithm without re-orthogonalization is reliable in our calculation. The shift-and-inverse Lanczos recursion is very efficient in solving large-scale eigenproblems, such as ideal MHD stability analysis in this paper. It provides a possible tool for us to work with more complicate problems. The detail description for ballooning modes in the three dimensional MHD equilibria will be given elsewhere.

Acknowledgements

Calculations have been carried on SX computer system in National Institute for Fusion Science (NIFS), Japan. The author (J. Chen) acknowledges with gratitude Dr Z.Bai in University of Kentucky for useful discussions. We are greatly indebted to Prof. J.Nührenberg and Dr C. Nührenberg for providing us the CAS3D2MN code to perform this work.

References

[1] C. Schwab, Ideal magnetohydrodynamics: global mode analysis of three-

dimensional plasma configurations. *Phys. Fluids* B**5**. 9(1993).

[2] D.V.Anderson, W.A.Cooper. R.Gruber. S.Merazzi, and U.Schwenn. Method for the efficient calculation of the (MHD) magnetohydrodynamic stability properties of magnetically confined fusion plasmas, *Int. J. Supercomput. Appl.* **4**. 3(1990).

[3] G. H. Golub and C. F. van Loan. Matrix Computations, 3rd Ed.. The Johns Hopkins University Press. (1996).

[4] B.S.Garbow, J.M.Boyle. J.J.Dongarra, C.B.Moler. EISPACK Guide, *Lecture Notes in Computer Science* **51**, 2nd Ed., Springer. New York (1977).

[5] E.Anderson, Z.Bai. C.Bischof, J.Demmel, J.Dongarra, J.DuCroz, A.Greenbaum, S.hammarling, A.McKennev, S.Ostrouchov, and D.Sorenson, *LAPACK Users' Guide, Release 2.0*, 2nd ed., SIAM Publications, Philadelphia (1995).

[6] C. C. Paige, Computational variants of the Lanczos method for the eigenproblem, *J. Inst. Math. Appl.* **10**, (1972). p.373.

[7] J. K. Cullum and R. A. Willoughby, *Lanczos algorithms for large symmetric eigenvalue computations, volume 1, Theory, Volume 2, Programs* (Birkhauser, Boston 1985).

[8] J. Cullum and R. A. Willoughby. Computing eigenvalues of very large symmetric matrices - an implementation of a Lanczos algorithm with no reorthogonalization, J. Comput. Physics. **44**. (1981). p.329.

[9] J. H. Chow, J. K. Cullum and R. A. Willoughby, A sparsity-based technique for identifying slow-coherent areas in large power systems, IEEE Trans. **PAS-103**, (1984), p.463.

[10] van Kats, J. M. and H. A. van der Vorst, Numerical results of the Paige-style Lanczos method for the computation of extreme eigenvalues of large sparse matrices, *Acad. Comp. Centrum Report* **TR-3**, (U. Utrecht 1976).

[11] van Kats, J. M. and H. A. van der Vorst, Automatic monitoring of Lanczos schemes for symmetric or skew symmetric generalized eigenvalue problems, *Acad. Comp. Centrum Report* **TR-7**, (U. Utrecht 1977).

[12] J. T. Edwards, D. C. Licciardello, and D. J. Thouless, Use of the Lanczos method for finding complete sets of eigenvalues of large sparse matrices, *J. Inst. Math. Appl.* **23**, (1979), p.277.

[13] B. N. Parlett, and J. K. Reid, Tracking the progress of the Lanczos algorithm for large sparse matrices, *IMA J. Numer. Anal.* **1**, (1981) p.135.

[14] A. Iiyoshi, M.Fujiwara, O.Motojima. N.Oyabu, and K. Yamazaki, *Fusion Technol.* **17**, (1990).

[15] N. Nakajima, *Physics of Plasmas* **3**, (1996), p.4545.

[16] N. Nakajima, *Physics of Plasmas* **3**, (1996), p.4556.

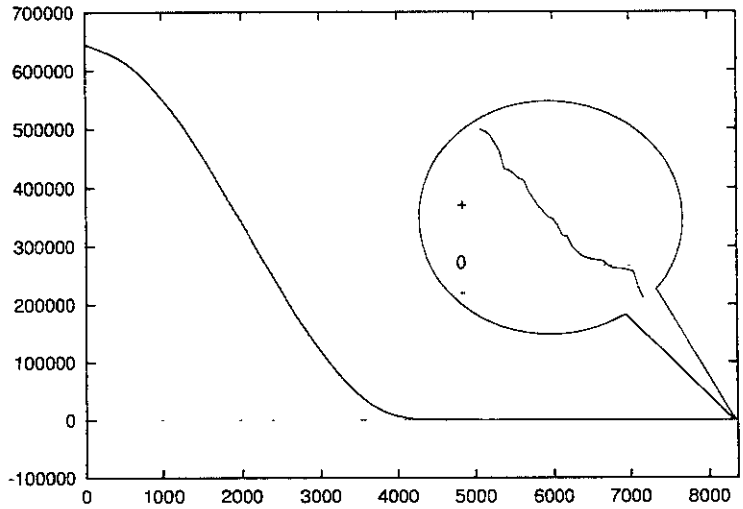

Figure 1. The distribution of MHD spectrum for a three dimensional MHD equilibria obtained by CAS3D2MN. The perturbation belongs to the $N = 5$ mode family with the phase factor $(M, N) = (8, -5)$. The radial mesh number NS is 120, and the total Fourier mode number L is 35. $\lambda_{min} = -2.14952 \times 10^{-3}, \lambda_{max} = 6.47634 \times 10^{6}$, $S(\boldsymbol{A}) = 8.70109 \times 10^{7}$. The positive eigenvalues are dominant and the negative eigenvalues are small in number and magnitude.

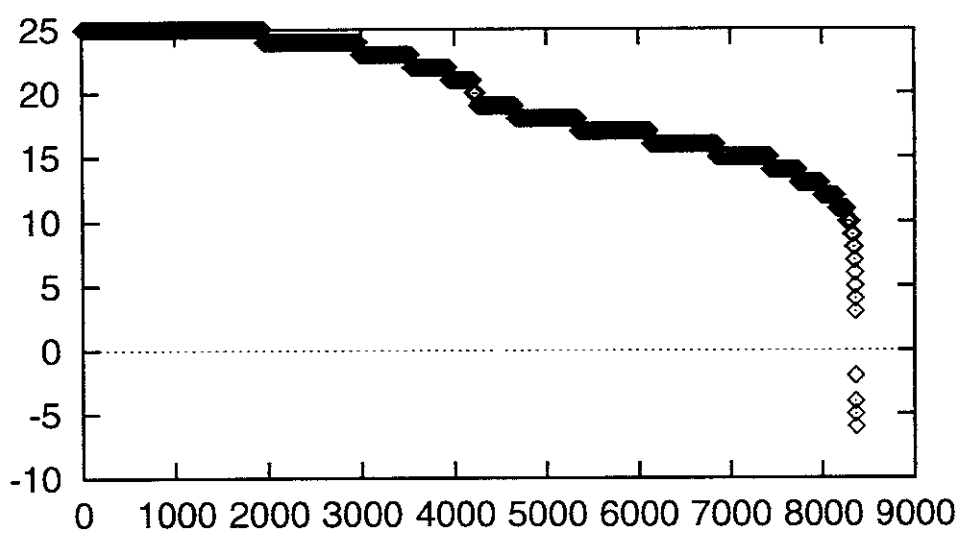

Figure 2. Scaled MHD spectrum of Fig.1 by $\sinh^{-1}(\alpha x)$ with $\alpha = 10^5$.

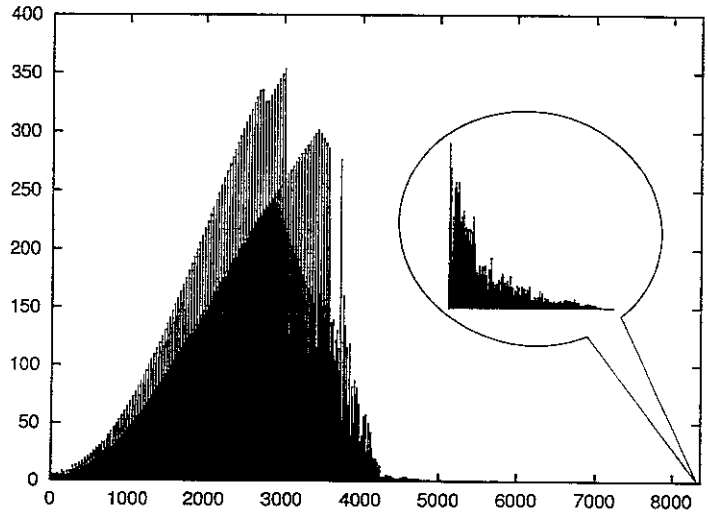

Figure 3. Gap stiffness for spectrum in Figs.1 and 2, where $g_{min} = 4.07164 \times 10^{-6}$, $g_{max} = 3.54277 \times 10^{2}$, and $S_g(\boldsymbol{A}) = 8.70109 \times 10^{7}$. The Lanczos steps m in Eg.(2.1) for λ_{min} is $11n$.

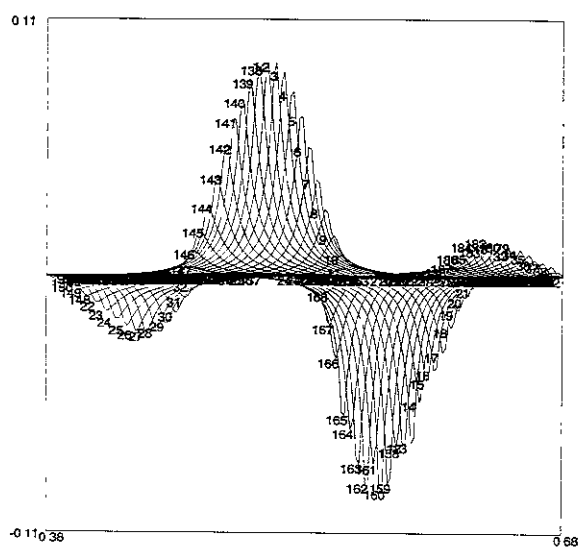

Figure 4. Ballooning mode in the strongly Mercier unstable three dimensional MHD equilibria, where $(M, N) = (133, -77)$, $(NS, L) = (600, 273)$. There are 4 groups with different toroidal mode numbers. From left to right, the toroidal mode number of each group is -67, -77, -87, and -97. The corresponding poloidal mode numbers for each group are from 137 to 123, from 143 to 123, from 143 to 123, and from 142 to 126, respectively.

Table 1.$(M, N) = (8, -5)$

(NS, L)	$\lambda_{min}(\times 10^{-3})$	Order (n)	storage (MB)	CPU(sec)	S_p	Algorithm
(120, 35)	-2.14952	8435	35	170.38		EISPACK
		8435	18	367.39		LAPACK
		20	11	3.14	54.25	(3.4)
(180, 35)	-1.97229	12635	94	374.52		EISPACK
		12635	25	585.76		LAPACK
		30	15	5.26	71.20	(3.4)
(120, 59)	-2.44352	14219	59	926.94		EISPACK
		14219	43	1703.05		LAPACK
		20	24	11.88	78.03	(3.4)
(180, 59)	-2.29349	21299	81	2068.69		EISPACK
		21299	63	2688.61		LAPACK
		20	34	16.75	123.50	(3.4)
(120, 109)	-2.92962	26269	147	2054.04		EISPACK
		26269	136	10500.86		LAPACK
		20	71	63.57	32.31	(3.4)
(240, 119)	-2.78503	57239	325	11242.46		EISPACK
		57239	-	34334.52		LAPACK
		20	163	150.12	74.89	(3.4)
(300, 201)	-2.90651	120801	-	-		EISPACK
		120801	-	-		LAPACK
		20	567	902.52	-	(3.4)

- means CPU times exceeds 10 hours.

Recent Issues of NIFS Series

NIFS-470 N. Nakajima, M. Yokoyama, M. Okamoto and J. Nührenberg,
Optimization of M=2 Stellarator; Dec. 1996

NIFS-471 A. Fujisawa, H. Iguchi, S. Lee and Y. Hamada,
Effects of Horizontal Injection Angle Displacements on Energy Measurements with Parallel Plate Energy Analyzer; Dec. 1996

NIFS-472 R. Kanno. N. Nakajima. H. Sugama, M. Okamoto and Y. Ogawa,
Effects of Finite-β and Radial Electric Fields on Neoclassical Transport in the Large Helical Device; Jan. 1997

NIFS-473 S. Murakami, N. Nakajima, U. Gasparino and M. Okamoto,
Simulation Study of Radial Electric Field in CHS and LHD; Jan. 1997

NIFS-474 K. Ohkubo, S. Kubo, H. Idei, M. Sato, T. Shimozuma and Y. Takita,
Coupling of Tilting Gaussian Beam with Hybrid Mode in the Corrugated Waveguide; Jan. 1997

NIFS-475 A. Fujisawa, H. Iguchi, S. Lee and Y. Hamada.
Consideration of Fluctuation in Secondary Beam Intensity of Heavy Ion Beam Prove Measurements; Jan. 1997

NIFS-476 Y. Takeiri. M. Osakabe, Y. Oka, K. Tsumori, O. Kaneko, T. Takanashi, E. Asano, T. Kawamoto, R. Akiyama and T. Kuroda,
Long-pulse Operation of a Cesium-Seeded High-Current Large Negative Ion Source; Jan. 1997

NIFS-477 H. Kuramoto, K. Toi, N. Haraki, K. Sato, J. Xu, A. Ejiri, K. Narihara, T. Seki, S. Ohdachi, K. Adati, R. Akiyama, Y. Hamada, S. Hirokura, K. Kawahata and M. Kojima,
Study of Toroidal Current Penetration during Current Ramp in JIPP T-IIU with Fast Response Zeeman Polarimeter; Jan., 1997

NIFS-478 H. Sugama and W. Horton,
Neoclassical Electron and Ion Transport in Toroidally Rotating Plasmas; Jan. 1997

NIFS-479 V.L. Vdovin and I.V. Kamenskij,
3D Electromagnetic Theory of ICRF Multi Port Multi Loop Antenna; Jan. 1997

NIFS-480 W.X. Wang, M. Okamoto, N. Nakajima, S Murakami and N. Ohyabu,
Cooling Effect of Secondary Electrons in the High Temperature Divertor Operation; Feb. 1997

NIFS-481 K. Itoh, S.-I. Itoh. H. Soltwisch and H.R. Koslowski,
Generation of Toroidal Current Sheet at Sawtooth Crash; Feb. 1997

NIFS-482 K. Ichiguchi,
Collisionality Dependence of Mercier Stability in LHD Equilibria with Bootstrap Currents; Feb. 1997

NIFS-483 S. Fujiwara and T. Sato,
Molecular Dynamics Simulations of Structural Formation of a Single Polymer Chain: Bond-orientational Order and Conformational Defects; Feb. 1997

NIFS-484 T. Ohkawa,
Reduction of Turbulence by Sheared Toroidal Flow on a Flux Surface; Feb. 1997

NIFS-485 K. Narihara, K. Toi, Y. Hamada, K. Yamauchi, K. Adachi, I. Yamada, K. N. Sato, K. Kawahata, A. Nishizawa, S. Ohdachi, K. Sato, T. Seki, T. Watari, J. Xu, A. Ejiri, S. Hirokura, K. Ida, Y. Kawasumi, M. Kojima, H. Sakakita, T. Ido, K. Kitachi, J. Koog and H. Kuramoto,
Observation of Dusts by Laser Scattering Method in theJIPPT-IIU Tokamak Mar. 1997

NIFS-486 S. Bazdenkov, T. Sato and The Complexity Simulation Group,
Topological Transformations in Isolated Straight Magnetic Flux Tube; Mar. 1997

NIFS-487 M. Okamoto,
Configuration Studies of LHD Plasmas; Mar. 1997

NIFS-488 A. Fujisawa, H. Iguchi, H. Sanuki, K. Itoh, S. Lee, Y. Hamada, S. Kubo, H. Idei, R. Akiyama, K. Tanaka, T. Minami, K. Ida, S. Nishimura, S. Morita, M. Kojima, S. Hidekuma, S.-I. Itoh, C. Takahashi, N. Inoue, H. Suzuki, S. Okamura and K. Matsuoka,
Dynamic Behavior of Potential in the Plasma Core of the CHS Heliotron/Torsatron; Apr. 1997

NIFS-489 T. Ohkawa,
Pfirsch - Schlüter Diffusion with Anisotropic and Nonuniform Superthermal Ion Pressure; Apr. 1997

NIFS-490 S. Ishiguro and The Complexity Simulation Group,
Formation of Wave-front Pattern Accompanied by Current-driven Electrostatic Ion-cyclotron Instabilities; Apr. 1997

NIFS-491 A. Ejiri, K. Shinohara and K. Kawahata,
An Algorithm to Remove Fringe Jumps and its Application to Microwave Reflectometry; Apr. 1997

NIFS-492 K. Ichiguchi, N. Nakajima, M. Okamoto,
Bootstrap Current in the Large Helical Device with Unbalanced Helical Coil Currents; Apr. 1997

NIFS-493 S. Ishiguro, T. Sato, H. Takamaru and The Complexity Simulation Group,

V-shaped dc Potential Structure Caused by Current-driven Electrostatic Ion-cyclotron Instability; May 1997

NIFS-494 K. Nishimura, R. Horiuchi, T. Sato,
Tilt Stabilization by Energetic Ions Crossing Magnetic Separatrix in Field-Reversed Configuration; June 1997

NIFS-495 T. -H. Watanabe and T. Sato,
Magnetohydrodynamic Approach to the Feedback Instability; July 1997

NIFS-496 K. Itoh, T. Ohkawa, S. -I.Itoh, M. Yagi and A. Fukuyama
Suppression of Plasma Turbulence by Asymmetric Superthermal Ions; July 1997

NIFS-497 T. Takahashi, Y. Tomita, H. Momota and Nikita V. Shabrov,
Collisionless Pitch Angle Scattering of Plasma Ions at the Edge Region of an FRC; July 1997

NIFS-498 M. Tanaka, A.Yu Grosberg, V.S. Pande and T. Tanaka,
Molecular Dynamics and Structure Organization in Strongly-Coupled Chain of Charged Particles; July 1997

NIFS-499 S. Goto and S. Kida,
Direct-interaction Approximation and Reynolds-number Reversed Expansion for a Dynamical System; July 1997

NIFS-500 K. Tsuzuki, N. Inoue, A. Sagara, N. Noda, O. Motojima, T. Mochizuki, T. Hino and T. Yamashina,
Dynamic Behavior of Hydrogen Atoms with a Boronized Wall; July 1997

NIFS-501 I. Viniar and S. Sudo,
Multibarrel Repetitive Injector with a Porous Pellet Formation Unit; July 1997

NIFS-502 V. Vdovin, T. Watari and A. Fukuyama,
An Option of ICRF Ion Heating Scenario in Large Helical Device; July 1997

NIFS-503 E. Segre and S. Kida,
Late States of Incompressible 2D Decaying Vorticity Fields; Aug. 1997

NIFS-504 S. Fujiwara and T. Sato,
Molecular Dynamics Simulation of Structural Formation of Short Polymer Chains; Aug. 1997

NIFS-505 S. Bazdenkov and T. Sato
Low-Dimensional Model of Resistive Interchange Convection in Magnetized Plasmas; Sep. 1997

NIFS-506 H. Kitauchi and S. Kida,

Intensification of Magnetic Field by Concentrate-and-Stretch of Magnetic Flux Lines; Sep. 1997

NIFS-507 R.L. Dewar,
Reduced form of MHD Lagrangian for Ballooning Modes; Sep. 1997

NIFS-508 Y.-N. Nejoh,
Dynamics of the Dust Charging on Electrostatic Waves in a Dusty Plasma with Trapped Electrons; Sep.1997

NIFS-509 E. Matsunaga, T.Yabe and M. Tajima,
Baroclinic Vortex Generation by a Comet Shoemaker-Levy 9 Impact; Sep. 1997

NIFS-510 C.C. Hegna and N. Nakajima,
On the Stability of Mercier and Ballooning Modes in Stellarator Configurations; Oct. 1997

NIFS-511 K. Orito and T. Hatori,
Rotation and Oscillation of Nonlinear Dipole Vortex in the Drift-Unstable Plasma; Oct. 1997

NIFS-512 J. Uramoto,
Clear Detection of Negative Pionlike Particles from H_2 Gas Discharge in Magnetic Field; Oct. 1997

NIFS-513 T. Shimozuma, M. Sato, Y. Takita, S. Ito, S. Kubo, H. Idei, K. Ohkubo, T. Watari, T.S. Chu, K. Felch, P. Cahalan and C.M. Loring, Jr,
The First Preliminary Experiments on an 84 GHz Gyrotron with a Single-Stage Depressed Collector; Oct. 1997

NIFS-514 T. Shjmozuma, S. Morimoto, M. Sato, Y. Takita, S. Ito, S. Kubo, H. Idei, K. Ohkubo and T. Watari,
A Forced Gas-Cooled Single-Disk Window Using Silicon Nitride Composite for High Power CW Millimeter Waves; Oct. 1997

NIFS-515 K. Akaishi,
On the Solution of the Outgassing Equation for the Pump-down of an Unbaked Vacuum System; Oct. 1997

NIFS-516 *Papers Presented at the 6th H-mode Workshop (Seeon, Germany)*; Oct. 1997

NIFS-517 John L. Johnson,
The Quest for Fusion Energy; Oct. 1997

NIFS-518 J. Chen, N. Nakajima, M. Okamoto,
Shift-and-Inverse Lanczos Algorithm for Ideal MHD Stability Analysis; Nov. 1997